Adaptive optics imaging system based on a high-resolution liquid crystal on silicon device

Quanquan Mu

State Key Lab of Applied Optics, Changchun Institute of Optics, Fine Mechanics and Physics, Chinese Academy of Sciences, Changchun, Jilin, 130033, China, and Graduate School of the Chinese Academy of Sciences, Beijing, 100039, China
muquanquan@ciomp.ac.cn

Zhaoliang Cao, Lifa Hu, Dayu Li, and Li Xuan

State Key Lab of Applied Optics, Changchun Institute of Optics, Fine Mechanics and Physics, Chinese Academy of Sciences, Changchun, Jilin, 130033, China

Abstract: An adaptive optics imaging system is introduced in this paper. A high-resolution liquid crystal on silicon (LCOS) device was used as a phase-only wavefront corrector instead of a conversional deformable mirror. The wavefront aberration was detected by a Shack-Hartmann (SH) wavefront sensor, which has a wavefront measurement accuracy of λ/100 rms (λ = 0.6328 μm). Under this construction, Peak-to-Valley correction precision of 0.09 λ was reached. Furthermore, some low-frequency hot convection turbulence induced by an electric iron was compensated in real time at the same precision. The modulation transfer function (MTF) of this system was also measured before and after wavefront correction. Under the active correction of LCOS, the system reached the diffraction limited resolution approximately 65l p/mm on the horizontal direction. All of this showed the possibility of using this device in a high-resolution, low temporal turbulence imaging system, such as retinal imaging, to improve the resolution performance.

OCIS codes: (230.3720) Liquid-crystal devices; (010.1080) Adaptive optics; (230.6120) Spatial light modulators

References and links

1. D. J. Cho, S. T. Thurman, J. T. Donner, and G. M. Morris, "Characteristics of a 128×128 liquid crystal spatial light modulator for wave-front generation," Opt. Lett. **23**, 969–971 (1998).
2. S. R. Restaino, D. M. Payne, J. T. Baker, J. R. Andrews, S. W. Teare, G. C. Gilbreath, D. Dayton, and J. Gonglewski, "Liquid crystal technology for adaptive optics: un update," SPIE **5003**, 187–192 (2003).
3. L. Hu, L. Xuan, Y. Liu, Z. Cao, D. Li, and Q. Mu, "Phase-only liquid crystal spatial light modulator for wave-front correction with high precision," Opt. Express **12**, 6403–6409 (2004).
4. H. Huang, T. Inoue, and T. Hara, "An adaptive wavefront control system using a high-resolution liquid crystal spatial light modulator," SPIE **5639**, 129–137 (2004).
5. K. A. Bauchert, S. A. Serati, and A. Furman, "Advances in liquid crystal spatial light modulators," SPIE **4734**, 35–43 (2002).
6. A. Kirby and G. Love, "Fast, large and controllable phase modulation using dual frequency liquid crystals," Opt. Express **12**, 1470–1475 (2004).
7. S. R. Restaino, D. Dayton, S. Browne, J. Gonglewski, J. Baker, S. Rogers, S. Mcdermott, J. Gallegos, and M. Shilko, "On the use of dual frequency nematic material for adaptive optics systems: first results of a closed-loop experiment," Opt. Express **6**, 2–6 (2000).
8. G. D. love, "Liquid crystal phase modulator for unpolarized light," Appl. Opt. **32**, 2222–2223 (1993).
9. T. L. Kelly and G. D. Love, "White-light performance of a polarization-independent liquid crystal phase modulator," Appl. Opt. **38**, 1986–1989 (1999).
10. D. Dayton, J. Gonglewski, S. Restaino, J. Martin, J. Phillips, M. Hartman, P. Kervin, J. Snodgress, S. Browne, N. Heimann, M. Shilko, R. Pohle, B. Carrion, C. Smith, and D. Thiel, "Demonstration of new technology MEMS and liquid crystal adaptive optics on bright astronomical objects and satellites," Opt. Express **10**, 1508–1519 (2002).

#71886 - $15.00 USD Received 12 June 2006; revised 24 July 2006; accepted 27 July 2006

11. Q. Mu, Y. Liu, L. Hu, D. Li, Z. Cao, and L. Xuan, "Determination of anisotropic liquid crystal layer parameters by spectroscopic ellipsometer," Acta Phys. Sin. **55**, 1055–1060 (2006).
12. Y. Liu, L. Xuan, L. Hu, Z. Cao, D. Li, Q. Mu, and X. Lu, "Investigation on the liquid crystal spatial light modulator with high precision and pure phase," Acta Opt. Sin. **25**, 1682–1686 (2005).
13. Y. Liu, L. Hu, Z. Cao, D. Li, Q. Mu, X. Lu, and L. Xuan, "The investigation of Controllable Phase liquid crystal spatial light modulator," Acta Photon. Sin. **34**, 1799–1802 (2005).
14. Y. Liu, L. Xuan, L. Hu, Z. Cao, D. Li, Q. Mu, and X. Lu, "The wavefront modulation characteristics of the parallel aligned liquid crystal device," Acta Photon. Sin. **35**, 65–68 (2006).
15. Z. Cao, L. Xuan, L. Hu, Y. Liu, and Q. Mu, "Effects of the space–bandwidth product on the liquid-crystal kinoform," Opt. Express **13**, 5186–5191 (2005).
16. C. Boyer, V. Michau, and G. Rousset, "Adaptive optics: interaction matrix measurements and real time control algorithms for the COME-ON project," SPIE **1237**, 406–421 (1990).

1. Introduction

Most available adaptive optics systems consist of a deformable mirror, which is very expensive and difficult to fabricate. In recent years, people in many countries have started using other devices such as the membrane deformable mirror and liquid crystal spatial light modulator (LC SLM) to replace the conventional deformable mirror and build a lower–cost, efficient adaptive optics system for many applications. It has been demonstrated that LC SLM can provide a convenient and effective means of amplitude or phase modulation [1]. Compared with the deformable mirror, the LC SLM has the advantages of low cost, reliability, low power consumption, low price, no moving mechanical components, and high resolution, as mentioned in several papers [2-5]. However, there are some drawbacks for liquid crystal devices, such as low temporal response, polarization dependence and dispersion. The response time and polarization dependence have been overcome with dual-frequency liquid crystal [6-7] and quarter wave plate [8-9], respectively. Some LC SLM-based adaptive optics systems have had very effective performance in astronomy [10], and they exhibit the enormous potential for using liquid crystal devices in wavefront correction.

Through former studies in our lab we have also demonstrated that liquid crystal can be used for phase modulation [11], and we have made a parallel-aligned LC SLM [12-14]. However, technical drawbacks of the LC SLM, related to its large pixel size and modulation depth less than 2 pi, restricted its performance in phase modulation, and a large modulation depth could not be achieved [15]. In this paper we introduce an adaptive optics imaging system based on an LCOS device, which is a micro display technology that has been used mostly in large-screen, high-contrast, high-definition, rear projection televisions and personal head-mount displays. Because the liquid crystal on silicon (LCOS) device has a small pixel pitch and high pixel density, it can get a modulation depth of more than 2 π in a wide wavelength range (from 400 nm to 700 nm). Such a system is beneficial to imaging operations with a small area, high precision, large modulation depth, and high resolution, such as retinal imaging. Therefore we intend to investigate its possible use in improving the imaging definition.

2. Adaptive optics imaging system

2.1 Experimental setup

The wavefront correction device used in this paper was an LCOS device called LCR2500 from Holoeye Corporation. Its phase stroke at wavelength of 0.6328 μm is 2.2 π without phase wrapping. With phase wrapping, its maximum phase stroke will be up to 200 π according to Ref. [15]. A Shack-Hartmann sensor (HASO32, Imagine Optic) was used to measure the wavefront aberration. The detailed parameters for both of them are shown in Table 1.

Figure 1 shows a schematic diagram of the optical layout. Light emitted from the tungsten lamp (white light) became horizontal polarized after passing through a polarizer, then collimated by lens L1 with focus of 500 mm and irradiated on the LCOS. The light reflected by the LCOS was refocused by L1. After passing through BS1 and BS2, the CCD would

#71886 - $15.00 USD Received 12 June 2006; revised 24 July 2006; accepted 27 July 2006

acquire an image of the filament. The filament is conjugated with the imaging plane of the CCD and the position of the hole. Another light beam transmitted through BS2 was collimated by L2 with focus of 100 mm and acquired by the HASO32 to measure the wavefront aberration induced by the roughness of the LCOS and the environment atmospheric turbulence. It should be noted that 960 × 720 pixels of LCOS were used in the experiment, which related to the 24 × 18 microlens of HASO32 because of the mask we made on the HASO32 and the zoom effect of lenses L1 and L2. The LCOS plane was conjugated with the microlens array plane of the HASO32.

The lens L1 has three main functions. First, when combined with the light source it is used to simulate an infinity object. The length of the filament was less than 1 mm, and the focus length of L1 was 500 mm, so it is similar to an object with a nearly 0.1° field angle. Second, it is considered as a telescopic lens. Last, L1 and L2 together are used to make the microlens array plane of the HASO32 be conjugated with the LCOS plane and match their pupil size.

Table 1. Detail parameters of LCR2500 and HASO32

(a) LCR2500

Parameter	Value	Unit
Active area dimensions	19.5 × 14.6	mm
Screen aspect ratio	4 (H) : 3 (V)	
Display resolution	1024 (H) × 768 (V)	pixels
Pixel pitch	19 x 19	μm
Pixel configuration	Orthogonal	
Gray levels	256 (8 bit)	
Optical efficiency Reflectance	> 75%	
Aperture ratio	> 93%	
Liquid crystal type	45° twisted nematic	
Polarizer mode	Normally black	
Max. refresh frame rate	75	Hz
Cell gap	5.5	μm
Phase stroke	1.1	λ(= 0.6328 μm)

(b) HASO32

Parameter	Value	Unit
Aperture dimension	5 × 5	mm^2
Number of subapertures	32 × 32	
Tilt dynamic range	>±3(520 λ)	°
Focus dynamic range	± 0,025 to ± ∞ (200 λ)	m
Repeatability (rms)	<1/200	wavelength
Wavefront measurement Accuracy in absolute mode (rms)	1/100	wavelength
Spatial resolution	~ 160	μm
Max. acquisition frequency	77	Hz

#71886 - $15.00 USD Received 12 June 2006; revised 24 July 2006; accepted 27 July 2006

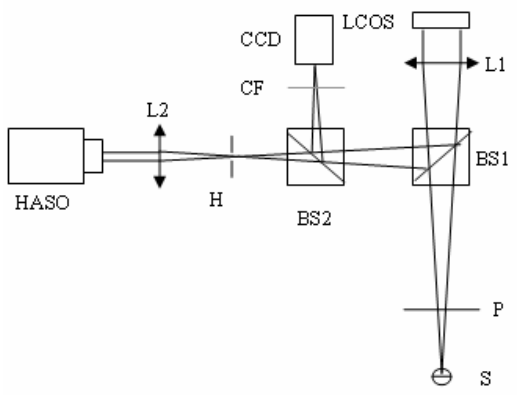

Fig. 1. Schematic diagram of the imaging system: S, light source; P, polarizer; BS, beam splitter; LCOS, liquid crystal on silicon; H, hole; HASO, wavefront sensor; CF, color filter.

2.2 Wavefront correction under low disturbance

Figure 2 shows the photograph of this experiment setup. The red line shows the ray path of light emitted from the tungsten lamp at the right side of the photo. A computer, not shown in this photo, is used to process the aberration signals detected by HASO32 and send the compensation command to the LCOS. The image of filament was recorded by a CCD camera. Because of the obvious dispersion of liquid crystal for white light, the liquid crystal wavefront corrector was able to correct the aberrated wavefront of light only in a narrow wavelength bandwidth range. In addition, the aberration detected by HASO32 was at the wavelength of 0.6328 μm. Therefore, to obtain a clear image, a color filter was inserted before the CCD camera to reject other wavelengths from the image.

An image of the filament before closed loop is shown in Fig. 3(a), and the related wavefront map is shown in Fig. 3(c). The aberration included here was mostly induced by the roughness of the LCOS and disturbances in the environment; it related to nearly 4.01λ PV and 0.851λ rms wavefront errors. An interaction matrix algorithm [16] was used to generate the compensation command. The Zernike polynomial was used to reconstruct the wavefront, and we used 36 Zernike modes here. Figs. 3(b) and 3(d) show the corrected image of the filament and the wavefront map, respectively. The temporal average residual aberration was 0.09λ PV and 0.016λ rms. The closed loop bandwidth was nearly 4 Hz under 0.8 closed loop gain. We can see that the image of the filament changed remarkably; the correction precision was very high. Due to the absence of strong dynamic turbulences, this result was very reliable and temporal stable.

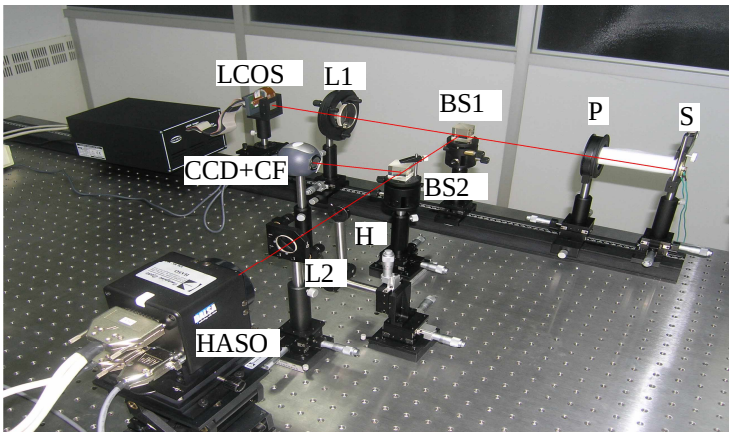

Fig. 2. Photograph of the optical layout in lab.

#71886 - $15.00 USD Received 12 June 2006; revised 24 July 2006; accepted 27 July 2006

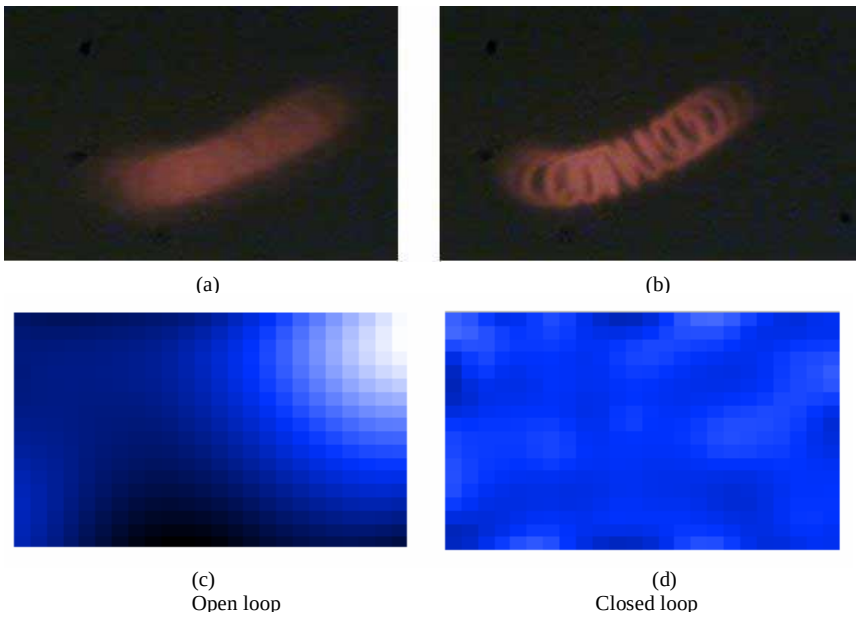

Fig. 3. Images of filament (a) open loop, (b) closed loop, and the wavefront map (c) open loop, (d) closed loop.

2.3 Wavefront correction under dynamic turbulence

In addition, the closed loop correction under dynamic turbulence has been conducted. An electric iron was used to induce hot convection in this optical system, which simulates low temporal frequency turbulence. Here, we only need qualitative analysis of effects due to turbulence. Therefore, turbulence was not quantified in the experiment. The electric iron is located between L1 and the LCOS, as shown in Fig. 4. The convection intensity can be adjusted by changing the distance between the electric iron and the optical axis. The image of filament was blurred and dithered before the loop was closed. When the correction began, it became clear and stable at once. The precision was the same as above. This process can be seen in the movie of Fig. 5.

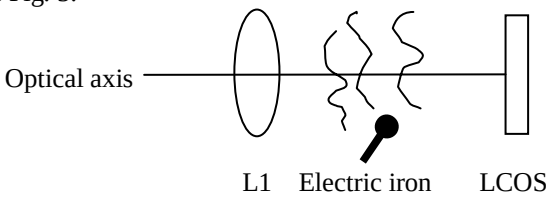

Fig. 4. Turbulence simulation.

Fig. 5. Closed loop correction under hot convection (1.01MB).

#71886 - $15.00 USD Received 12 June 2006; revised 24 July 2006; accepted 27 July 2006

To estimate the performance of this system, the modulation transfer function (MTF) was measured before and after correction. Figure 6 shows the MTF in the horizontal and vertical directions, respectively. This system approximately reached the diffraction limited performance after correction, especially in the 90° direction. The critical frequency increased from approximately 3l p/mm to almost 50l p/mm in the vertical direction and 65l p/mm in the horizontal direction. The resolution characteristic improved dramatically.

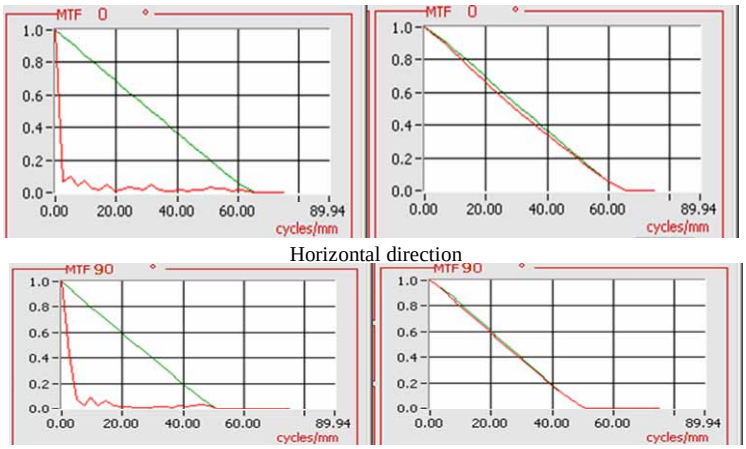

Horizontal direction

Vertical direction

(a) Open loop (b) Closed loop

Fig. 6. MTF of this imaging system.

3. Conclusion

LCOS devices have mostly been used in large-screen, high-contrast, high-definition, rear projection televisions and personal head-mount displays. Because they have a small pixel pitch and high pixel density, LCOS devices are mostly beneficial for small area, high precision, low temporal frequency, and high-resolution-phase only wavefront correction.

A high-resolution adaptive optics imaging system that is based on LCOS has been introduced in this paper. A Shack-Hartmann (SH) wavefront sensor was used to detect the wavefront aberration. The temporal averaged residual aberration after the closed loop correction was 0.09λ PV and 0.016λ rms under dynamic hot convection. The closed loop bandwidth was nearly 4 Hz at 0.8 closed loop gain. This bandwidth was narrow for astronomy but effective for other imaging systems that contain low temporal frequency turbulence, such as retinal imaging. Improving the bandwidth is still a significant task for the future. The MTFs of this demonstration system also have been measured, which showed the effectiveness of using the LCOS device to improve the performance of the imaging system. The critical frequency increased from approximately 3l p/mm to almost 50l p/mm in the vertical direction and 65l p/mm in the horizontal direction. LCOS will be applied to retinal imaging in the future.

Acknowledgments

This work is supported by National Natural Science Foundation (No. 60578035, No. 50473040) and Science Foundation of Jilin Province (No. 20050520, No. 20050321-2).

#71886 - $15.00 USD Received 12 June 2006; revised 24 July 2006; accepted 27 July 2006